AD A120481

DTIC FILE COPY

SECURITY CLASSIFICATION OF THIS PAGE (When Data Entered)

REPORT DOCUMENTATION PAGE

READ INSTRUCTIONS BEFORE COMPLETING FORM

1. REPORT NUMBER: 14 (12)	2. GOVT ACCESSION NO.: AD-A120481
3. RECIPIENT'S CATALOG NUMBER:	
4. TITLE (and Subtitle): ACOUSTICAL SCANNING OF OPTICAL IMAGES	5. TYPE OF REPORT & PERIOD COVERED: Semiannual Technical Report 1 January 1982 - 30 June '82
	6. PERFORMING ORG. REPORT NUMBER: GL 3478
7. AUTHOR(s): G. S. Kino, R. Thornton, J. B. Green	8. CONTRACT OR GRANT NUMBER(s): N00014-76-C-0129
9. PERFORMING ORGANIZATION NAME AND ADDRESS: Edward L. Ginzton Laboratory, W. W. Hansen Laboratories of Physics, Stanford University, Stanford, CA. 94305	10. PROGRAM ELEMENT, PROJECT, TASK AREA & WORK UNIT NUMBERS: PE 61101E, 8D10, Order No. 2778-5
11. CONTROLLING OFFICE NAME AND ADDRESS: Defense Advanced Research Projects Agency, DSO, 1400 Wilson Boulevard, Arlington, VA. 22209	12. REPORT DATE: August 1982
	13. NUMBER OF PAGES: 28
14. MONITORING AGENCY NAME & ADDRESS (if different from Controlling Office): Office of Naval Research, Code 414, 800 N. Quincy Street, Room 323, Arlington, VA. 22217	15. SECURITY CLASS. (of this report): Unclassified
	15a. DECLASSIFICATION/DOWNGRADING SCHEDULE

16. DISTRIBUTION STATEMENT (of this Report)

Approved for public release; distribution unlimited

DTIC ELECTE OCT 19 1982 D H

17. DISTRIBUTION STATEMENT (of the abstract entered in Block 20, if different from Report)

18. SUPPLEMENTARY NOTES

ONR Scientific Office
(202) 696-4218

19. KEY WORDS (Continue on reverse side if necessary and identify by block number)

SAW/FET, ZnO deposition, laser probe, sputter deposition, Schottky diode, acoustic surface wave devices, programmable storage correlator, shift register, FET array, insertion loss,

20. ABSTRACT (Continue on reverse side if necessary and identify by block number)

The fiber-optic laser probe has been used as a diagnostic tool to identify loss mechanisms in monolithic storage correlators, generating suggestions for improved device efficiency. Schottky diode correlators have been operated in the input correlation mode, demonstrating that it is possible to charge Schottky diodes slowly as p-n diodes with proper voltage amplitudes. Schottky diode correlator theory has been modified to account for charge leakage effects and comparisons with experimental results have been made. A new signal processing device, the SAW/FET, has been introduced which interfaces high-speed analog sig[illegible] with slow-speed digital ones. Experimental results are presented.

DD 1 JAN 73 1473 EDITION OF 1 NOV 65 IS OBSOLETE
S/N 0102-LF-014-6601

SECURITY CLASSIFICATION OF THIS PAGE (When Data Entered)

ACOUSTICAL SCANNING OF OPTICAL IMAGES

Semiannual Technical Report No. 14
1 January 1982 - 30 June 1982

Principal Investigator:

G. S. Kino
(415) 497-0205

Sponsored by
Defense Advanced Research Projects Agency
DARPA Order No. 2778

Contract N00014-76-C-0129
Program Code Number: 4D10
Contract Period: 1 July 1975 - 14 November 1983
Amount of Contract: $899,260
Form Approved, Budget Bureau - No. 22R0293

Approved for public release: distribution unlimited

Reproduction, in whole or in part, is permitted for any purpose of the U.S. Government.

The views and conclusions contained in this document are those of the authors and should not be interpreted as necessarily representing the official policies, either expressed or implied, of the Defense Advanced Research Projects Agency or the U.S. Government.

G. L. Report No. 3478

August 1982

Edward L. Ginzton Laboratory
W. W. Hansen Laboratories of Physics
Stanford University
Stanford, California 94305

I. SCHOTTKY DIODE STORAGE CORRELATORS

During the past six months we have directed our efforts at refining the fabrication process for wideband Schottky diode storage correlators. As mentioned in our last progress report, this effort was hindered somewhat by unexpected difficulties in our ZnO deposition process. The most severe of these difficulties have been overcome, and our efforts now are centered around increasing the transduction and delay line efficiencies of these devices.

We have utilized the fiber-optic laser probe to investigate the details of propagation in Sezawa mode surface wave delay lines. Due to the somewhat nonuniform deposition characteristics in the ZnO sputter deposition station, it is predictable but severe phase distortions occur across the acoustic beampath, resulting in greatly excessive insertion loss. This work is summarized in detail in the paper given as Appendix 1.* One important result is that the attenuation of the ZnO itself is of the order of 1 dB/cm at 165 MHz . Thus, we could expect to use these device concepts at considerably higher center frequencies and bandwidths.

The only solution to this problem is to maintain a high degree of ZnO thickness uniformity in the direction perpendicular to the acoustic propagation direction. In the present geometry of the ZnO deposition station, this means that the samples must be close in to the center of the circularly-symmetric distribution of ZnO thickness in the deposition plane. By accounting for the unavoidable losses in the delay line (bidirectionality, bulk wave excitation, and propagation loss), it appears possible to maintain the total insertion loss (in a 2 cm long Sezawa mode device at 160 MHz)

significantly below 20 dB . We are currently using the information provided by laser probe measurements to implement these design improvements.

We have demonstrated the ability of the Schottky diode correlator to operate in the slow-charging mode necessary to perform input correlation. Since Schottky diodes are capable of efficient storage within a single rf cycle of a sufficiently large rf pulse, the question has been raised as to whether the device is at all capable of storing slowly over many rf cycles, each of which gives a small increment of stored charge. Figure 1 shows the result of such an experiment, where the input voltage amplitudes were 4.2 volts on the acoustic port during read-in, 7 volts on the acoustic port during read-out, and 10 volts on the top-plate port. The input pulses were 0.2 ms in duration. Fig. 2 shows the dependence of the output pulse on the time duration of the top-plate and acoustic waveforms.

These results show that the Schottky diode correlator can indeed be operated in the input correlation mode. the maximum integration time being determined by the peak amplitude of the signal applied to the top-plate. We conclude from these experiments that the basic function of the Schottky diode correlator in this mode is very similar to that of the P-N diode correlator, provided that the input voltages are sufficiently small.

Due to the relatively poor storage time performance of the device we are working with at present (~1 ms) it remains to be seen whether the linear input correlation range can be extended from the several tens of microseconds range we have now demonstrated up into the several millisecond range that has been demonstrated in P-N diode correlators. We anticipate our next generation of devices having sufficient storage times to further investigate this issue.

We have developed a large signal theory to describe the charging characteristics as a function of applied read-in pulse amplitude in the Schottky diode correlator. Previously, this theory neglected the effect of charge leakage on the observed correlation output. We have found that this charge leakage is significant and must be considered in order to achieve reasonable agreement between theory and experimental observations. The difficulty is demonstrated in Figs. 3 a,b,c where the correlation output as a function of time is displayed for three different applied top-plate voltages. These three figures demonstrate that the effective storage time increases with the total amount of charge stored on the diode, and further that the envelope of the stored charge decay changes from an apparently exponential decay at small voltages to a more linear relation for larger voltages. In Fig. 4 we show the curves obtained for correlation output as a function of time when the theoretical reverse leakage of a Schottky diode is assumed, modified by an additional term to allow for excess reverse leakage.

It can be seen that the qualitative behavior of these curves is very similar to the experimental results we have measured. We have neglected thus far the effect of charge storage in surface states and series resistance. Inclusion of these effects could result in better agreement between theory and experiment.

DTIC COPY INSPECTED

Accession For
NTIS GRA&I
DTIC TAB
Unannounced
Justification
By
Distribution/
Availability Codes
Dist | Avail and/or Special
A

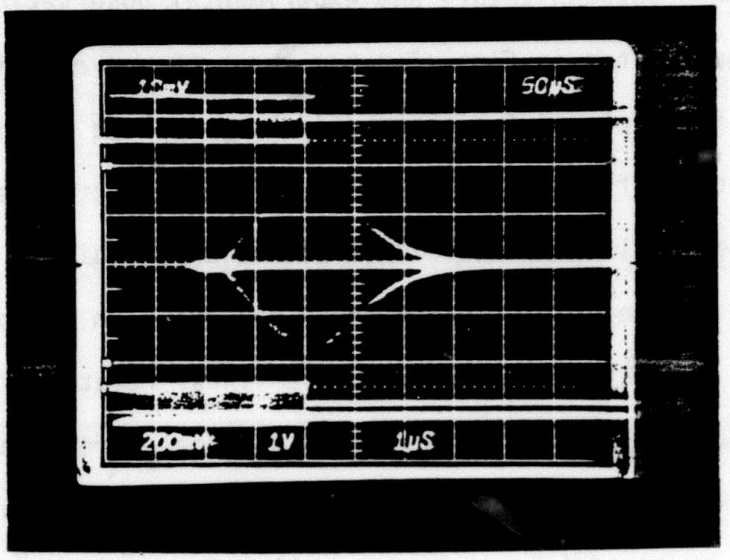

Fig. 1. Input correlation experiment - acoustic to plate readout. Upper trace: acoustic port signals (50 μsec/div). Middle trace: correlation output trace (1 μsec/div). Lower trace: top-plate signal (50 μsec/div).

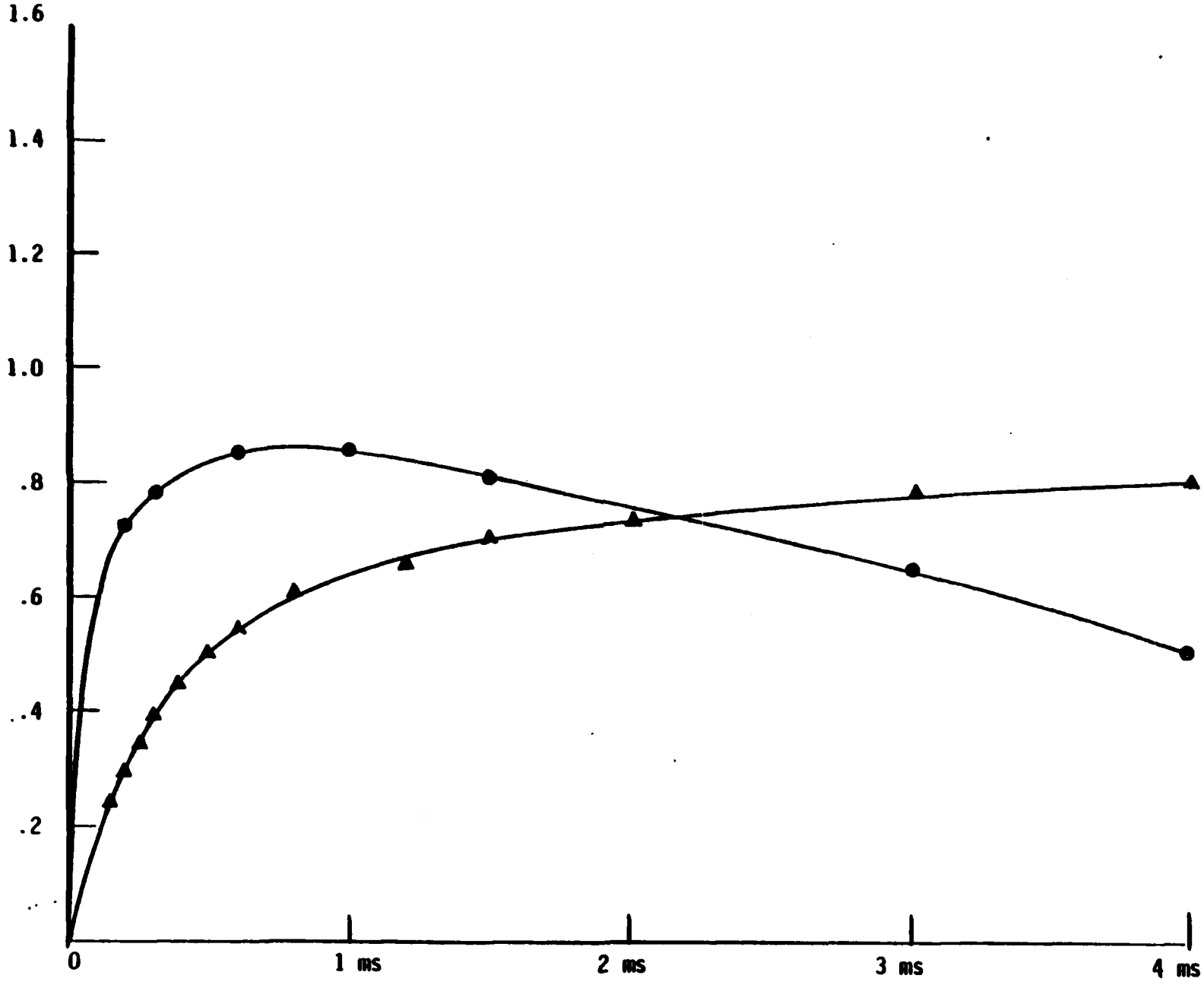

Fig. 2. Correlation output versus input correlation width at various voltages.

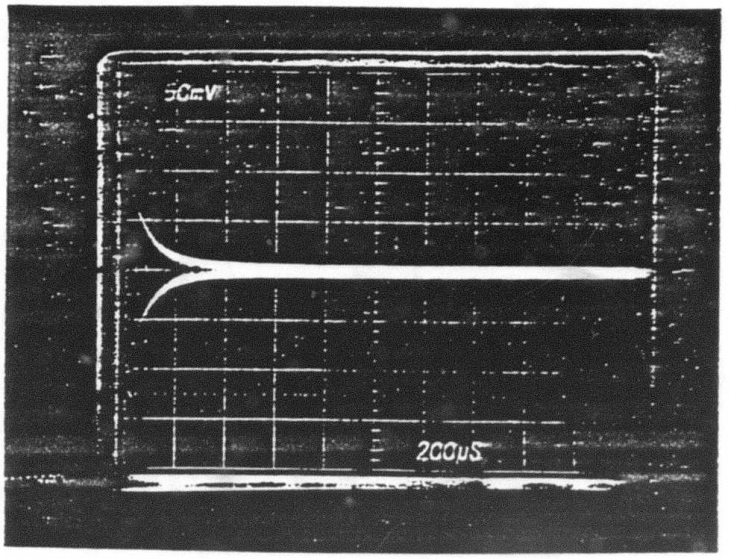

Fig. 3.

(a) 19.9 volts

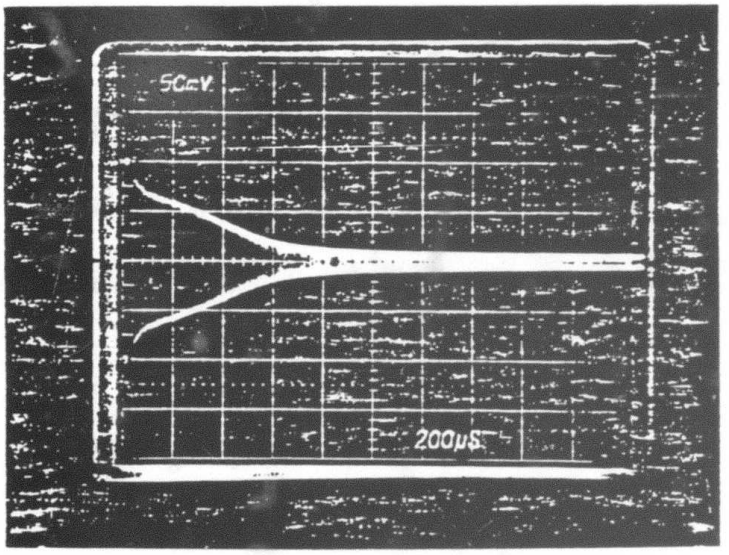

(b) 35.3 volts

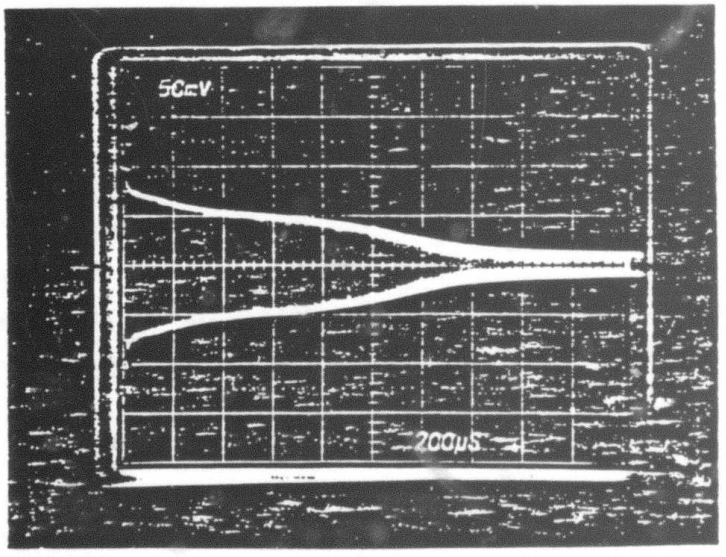

(c) 56 volts

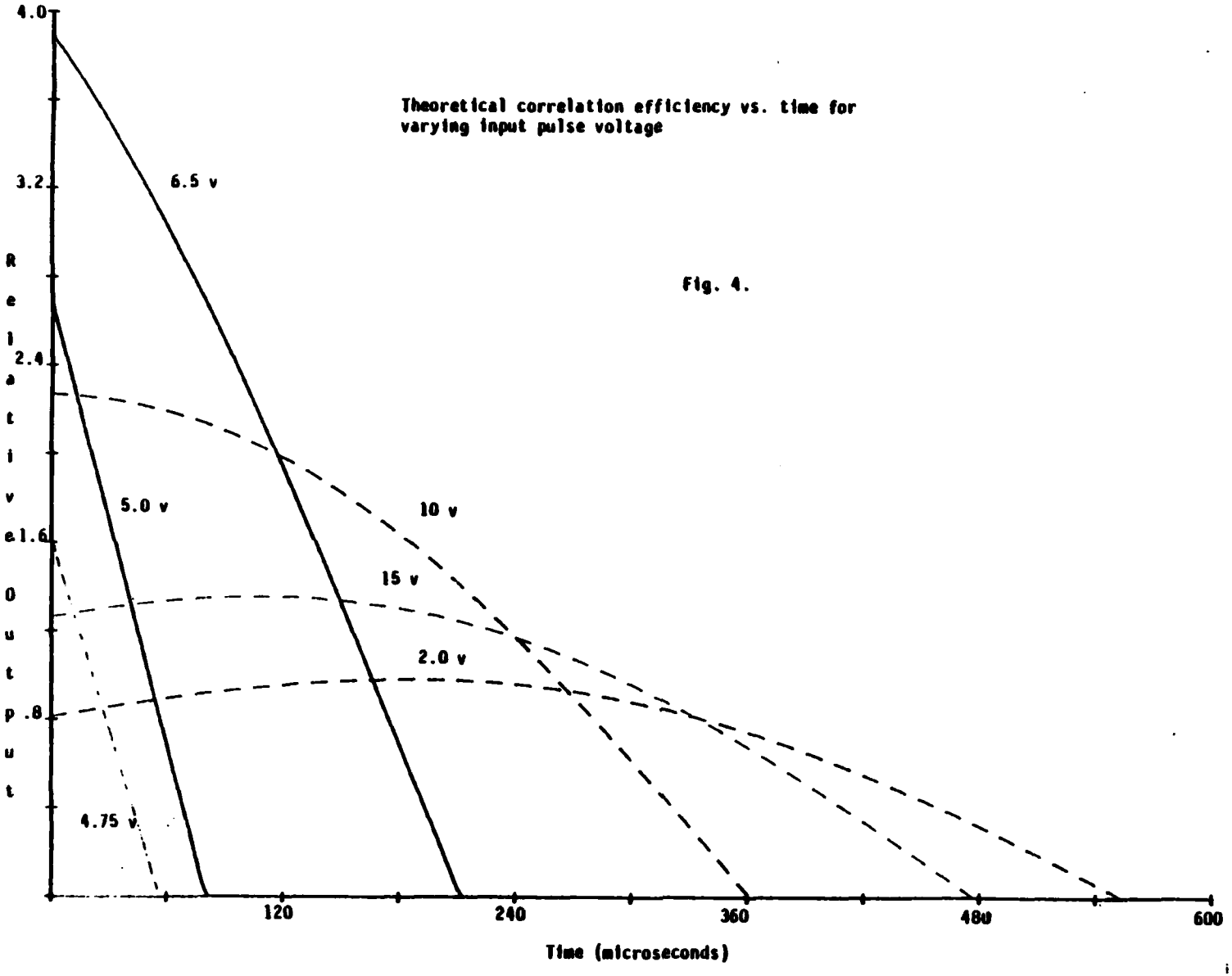

Theoretical correlation efficiency vs. time for varying input pulse voltage

Fig. 4.

II. THE SAW/FET - A NEW ANALOG SIGNAL PROCESSING DEVICE

A closely related extension of this ZnO/Si SAW device work has been carried out by J. B. Green under ONR contract N00014-75-C-0632. The thrust of this work involves the exploitation of the ZnO/Si structure to integrate with the surface wave device a more sophisticated electronic circuitry. We now intend to transfer this work to the present program because it fits so well with the basic aims of the project.

The work demonstrates that acoustic surface wave devices can be constructed on silicon and that sophisticated signal processing can be carried out by taking advantage of LSI technology. Thus, our aim is to demonstrate a marriage between LSI technology and acoustic surface wave technology, both in form and in function.

We have chosen to demonstrate our ideas by constructing a low-speed programmable storage correlator (which we have named the SAW/FET). The basic principles of operation of this devic (called the SAW/FET) follow directly from that of the storage correlator. Figure 5 shows a simplified view of the device. We see here that it is very similar to the storage correlator, except for the important difference that each diode is connected to a MOSFET, the drains of all the individual MOSFETS being connected to a common input-output line. The gates of the MOSFETS themselves are controlled by a shift register. We see that this device employs far more sophisticated semiconductor techniques than just the diffusion of simple diodes. It is capable of processing high-frequency signals (from the surface acoustic waves), while controlling the processing with relative low-frequency signals (by way of the shift register/multiplexed FET arrangement).

A low-speed waveform is inserted into the device by applying an analog signal $h(t)$ to the common drain line of the FET array while simultaneously clocking the single bit tapped shift register. It can be seen that when the multiplexed FETs are switched on by the tapped shift register, a different sample of the analog waveform is stored in successive diodes in the array. The waveform samples are stored as charge on the reverse-biased diodes so that this array of reverse-biased diodes has a capacitance variation $C(z)$ along the length of the device that is representative of the original analog input signal $h(t)$. The z-direction is defined to be along the device length, colinear with the direction of propagation of the surface acoustic waves. Operation of this device in the plate-to-acoustic readout mode is identical to the storage correlator. However, the output will be large only when $C(z) = M(z) \cos kZ$, where $k = \omega/v_a$ and v_a is the surface acoustic wave propagation velocity.

Figure 6 shows the correlation output of a 96 MHz modulated 3-bit Barker code (++-) with a low-frequency modulated 3-bit Barker code previously stored in the device. The peak-to-sidelobe ratio is seen to equal 3/1 , the expected value for the autocorrelation of a 3-bit Barker code.

In both of the above demonstrations the reference programming time was approximately 2 msec . This programming time can be reduced by clocking the shift register circuitry at an appropriately higher speed. The fastest observed operation of the shift registers has indicated that reference programming times as short as 35 μsec can be obtained.

Reference holding times were not measured, yet it is fully expected that they are on the order of tens of milliseconds, similar to the room temperature

storage time of the ZnO/Si storage correlator. By cooling the device, this storage time can be increased up to several minutes.

The peak signals are observed to be 23 dB above the acoustically generated spurious signal. These spurious signals are due to acoustic feedthrough caused by non-uniformities in the zinc oxide layer. There also exist strong capacitive feedthrough signals picked up by the interdigital transducers which are located close to the plate electrode. We believe that these non-uniformities and pick-up problems can be minimized by a slight modification of the FET array processing schedule, and by placing ground metallizations between the interdigital transducers and the top-plate electrode. This will be done in subsequent devices, hopefully resulting in a much larger dynamic range.

The five finger pair interdigital transducers were tuned using a lumped element BALUN network. At a center frequency of 101 MHz , the device had an rf delay line insertion loss of -33 dB with a 3 dB bandwidth of 11 MHz . Accounting for electrical mismatch loss and the bidirectionality of the interdigital transducers, it is calculated that the surface acoustic wave loss across the interaction region is less than .02 dB/tap .

It must also be noted that this present device has a processing bandwidth limited only by the interdigital transducers. Since the high tap density allows the processing of signals with bandwidths in excess of 200 MHz , improved device performance can be obtained by utilizing higher frequency transducers operating in the Sezawa mode to achieve greater IDT bandwidths [8].

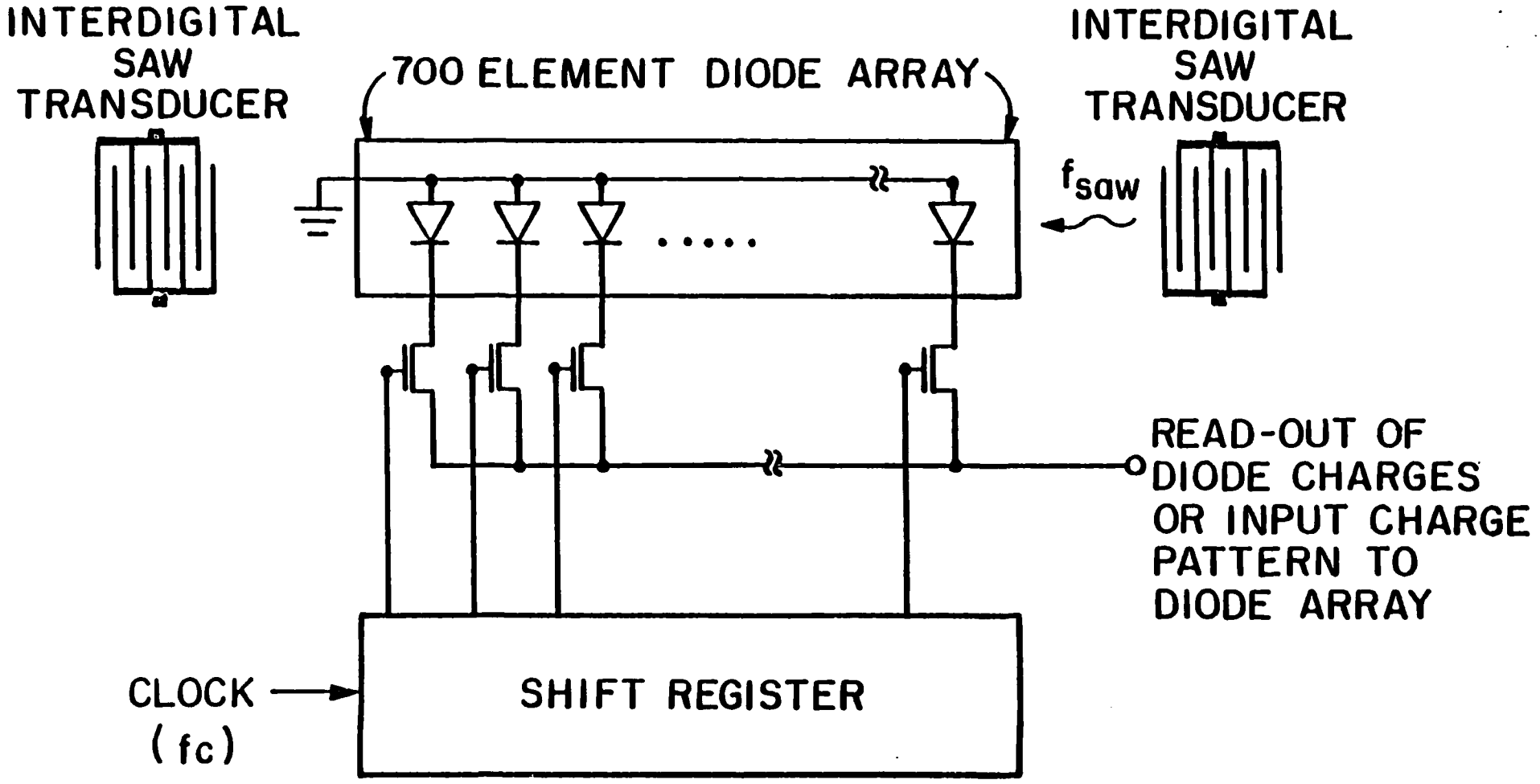

$f_{saw} >> fc$

SCHEMATIC OF SAW/FET DEVICE

Fig. 5.

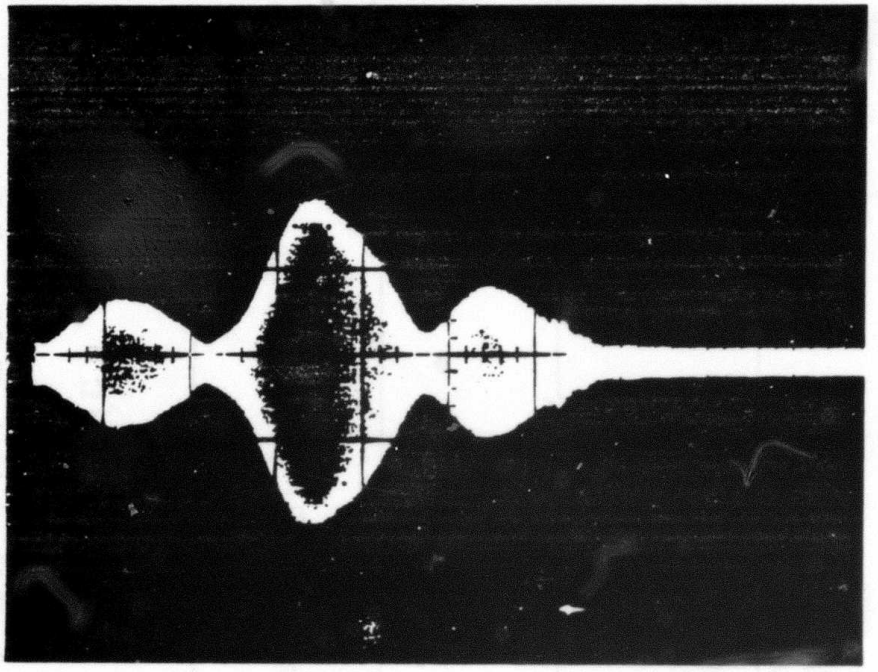

Fig. 6. Correlation output of two 3-bit Barker codes (++-). Horizontal scale: .1 μsec/div.

Appendix I

THE EFFECT OF NONUNIFORM PIEZOELECTRIC FILMS ON MONOLITHIC SURFACE ACOUSTIC WAVE DEVICES

by

J. E. Bowers, R. L. Thornton, B. T. Khuri-Yakub,

R. L. Jungerman, and G. S. Kino

Preprint

G.L. Report No. 3420

Revised, August 1982

ONR N00014-76-C-0129

Submitted to Applied Physics Letters

Edward L. Ginzton Laboratory
W. W. Hansen Laboratories of Physics
Stanford University
Stanford, California 94305

THE EFFECT OF NONUNIFORM PIEZOELECTRIC FILMS ON MONOLITHIC SURFACE ACOUSTIC WAVE DEVICES

ABSTRACT

The effect of film thickness variation on the performance of ZnO on silicon surface acoustic wave delay lines is examined. The thickness variation obtained from a planar magnetron sputtering system with a 5 cm diameter erosion ring was measured and found to be in good agreement with the calculated thickness variation. This information, together with theoretical data on the dependence of surface acoustic wave velocity on ZnO film thickness, is used to predict phase distortions of 400° across 1 mm wide 2.5 cm long delay lines. This high level of phase distortion was confirmed by experimental measurements with a laser probe.

Extensive research has been conducted on the development of monolithic surface acoustic wave (SAW) devices that utilize a piezoelectric thin film deposited on a substrate that has some desired property such as semiconductor effects, low cost, or temperature stability. The piezoelectric films are typically ZnO or AlN. Sputtering onto heated substrates has been the most successful approach for obtaining oriented films [1-3]. Moving the substrate during the deposition causes some difficulty in monitoring the substrate temperature and maintaining a constant substrate temperature. Consequently, most depositions are made on stationary samples. It will be shown in this paper that the resulting thickness variations cause significant deleterious effects on many SAW devices such as delay lines, filters, convolvers and memory correlators. Phase distortion due to the variation of surface wave velocity across the surface will be investigated by considering: (1) the dependence of phase velocity on film thickness; and (2) the dependence of film thickness on radial position from the sputtering axis.

The dependence of phase velocity on ZnO film thickness is shown in Fig. 1 for the first two Rayleigh modes on a <100> silicon substrate. The positions of the maxima of the SAW coupling coefficient are indicated in the figure [4]. Similar curves for ZnO films on other substrates are given in [5,6], and analogous curves for AlN films on various substrates are given in [7,8]. Experimental results will be presented for the second Rayleigh mode (Sezawa mode). It can be seen that the slope of the velocity versus thickness curve for the Sezawa mode is slightly less than the slope for the fundamental Rayleigh mode at the position of the first $\Delta v/v$ peak. Consequently, the latter devices will have more phase distortion than Sezawa mode devices. The

least distortion is obtained with fundamental Rayleigh mode devices using the second $\Delta v/v$ maximum.

A typical thickness variation across a 4 cm by 4 cm wafer is shown in Fig. 2a, where the interference fringes of 5400 Å light can be seen. The ZnO film was deposited using planar magnetron sputtering with a 5.2 cm diameter erosion ring. The substrate-to-target spacing was 4.2 cm . The thickness variations are typically worse if smaller samples are used since the clamps holding the sample often affect the deposition pattern (Fig. 2b).

The thickness variation across two 4 cm by 4 cm samples were measured and plotted in Fig. 3. Also plotted are the theoretical predictions based on a $\cos\theta$ sputtering distribution [9] from an annulus 8 mm wide with a diameter of 5.2 cm . This annulus corresponds to the dimensions of the erosion ring in the target after extensive sputtering. A target-to-substrate spacing of 3.5 cm results in the flattest distribution over the central 2 cm by 2 cm region. A spacing of 5 cm , which results in better film orientation than 3.5 cm spacing, produces the other thickness distribution shown in Fig. 3.

The phase distortion of a surface acoustic wave can be calculated from the information in Figs. 1 and 3. The difference in phase across the receiving transducer is, to first order in the transducer width Δy ,

$$\Delta\phi = \omega\Delta y \int_0^L \frac{1}{v(h)^2} \frac{dv(h)}{dh} \frac{dh}{dy}\, dx \qquad (1)$$

where ω is the acoustic frequency, h is the film thickness, and L is the distance between IDTs. For a thin erosion ring of radius s , the thickness distribution across the film is

$$\frac{h}{h_0} = \frac{[1 + (r/\ell)^2 + (s/\ell)^2][1 + (s/\ell)^2]^2}{\{[1 - (r/\ell)^2 + (s/\ell)^2]^2 + 4(r/\ell)^2\}^{3/2}} \qquad (2)$$

when h_0 is the thickness at the center, r is the radial distance from the target axis ($r^2 = x^2 + y^2$) and ℓ is the substrate-to-target spacing. Using Eq. (2) in Eq. (1) and calculating the integral numerically, the phase distortion across a transducer can be calculated as a function of the distance (y) from the target axis to the center of the acoustic beam. This is shown in Fig. 4 for several substrate-to-target spacings. The distortion is 300-400° for devices that are 2 cm from the target axis. This results in an additional loss of 20 dB . Only a few devices close to the target axis will have low insertion loss.

The severe phase distortions described above have been measured with a fiber optic SAW sensor [10]. The sample was a Sezawa wave storage correlator with 8 μm of ZnO deposited on 2000 Å of SiO_2 on <100> Si. The IDTs were 1 mm wide. The ZnO film was deposited with a target-to-substrate distance of 4 cm and the sample was 2 cm from the center axis of the target. The acoustic amplitude and phase at the transmitting transducer are shown in Fig. 5a. The same measurement 2 cm closer to the receiving transducer (Fig. 5b) shows that significant beam steering or diffraction did not occur. The average acoustic amplitude is .55 times the amplitude at the transmitting transducer, indicating that the total loss due to ZnO attenuation, interaction with carriers in the silicon, beamsteering and diffraction are less than 6 dB . The phase variation at the receiving transducer is 500° , resulting in a theoretical loss of 12 dB (calculated

assuming a linear phase variation of 500° across the transducer). Thus, we expect 6 dB of loss due to attenuation and 12 dB of loss due to phase distortion resulting in a total excess loss of 18 dB . The experimentally measured difference in insertion loss between short (.4 cm) and long (2.5 cm) delay lines on this sample was found to be 15 dB .

Phase distortion and its effect on delay line loss has been described. Similar problems occur in convolvers since the phase fronts of the counterpropagating waves are affected in opposite ways. Similarly, memory correlators used in applications that utilize both IDTs have similar distortion problems. However, memory correlators will not be adversely affected provided that only one IDT is used for the write and read operations and provided that multiple diodes across the beamwidth are used so that averaging of the phase fronts does not occur.

One solution to the thickness variation problem is to move the sample during the deposition. Other solutions would be to use a larger target with larger magnets or to use just a few devices close to the target axis. If the excess loss of a 2 cm long, 1 mm wide delay line is to be less than 2 dB , then the phase distortion must be less than 130° for a 30 λ beamwidth transducer. This means that only samples within 1.2 cm of the target axis can be used (for s = 3.5-4 cm). A final solution is to use a different sputtering system than a planar magnetron system, such as dc triode or rf diode, which have more uniform deposition patterns.

ACKNOWLEDGMENT

This work was supported by the Defense Advanced Research Projects Agency and monitored by the Office of Naval Research under Contract No. N00014-76-C-0129.

REFERENCES

1. T. Yamamoto, T. Shiosaki, and A. Kawabata, J. Appl. Phys. 51, 3113 (1980).
2. B. T. Khuri-Yakub and J. G. Smits, "Reactive Magnetron Sputtering of ZnO," Ultrasonics Symp. Proc., 801 (1980).
3. F. S. Hickernell, "ZnO Processing for Bulk and Surface Wave Devices," Ultrasonics Symp. Proc., 784 (1980).
4. J. E. Bowers, B. T. Khuri-Yakub, and G. S. Kino, "Broadband Efficient Thin Film Sezawa Wave Interdigital Transducers," Appl. Phys. Lett. 10, 806 (1980).
5. G. S. Kino and R. S. Wagers, "Theory of Interdigital Couplers on Nonpiezoelectric Substrates," J. Appl. Phys. 44, 1480 (1973).
6. T. W. Grudkowski, G. S. Montress, M. Gilden, and J. F. Black, "GaAs Monolithic SAW Devices for Signal Processing and Frequency Control," Ultrasonics Symp. Proc., 88 (1980).
7. T. Shiosaki, K. Harada, and A. Kawabata, "Low Temperature Growth of the Piezoelectric AlN Film and Its Optical and Acoustic Properties," Ultrasonics Symp. Proc., 506 (1981).
8. K. T. Subouchi, K. Sugai, and N. Mikoshiba, "ALN Materials Constants Evaluation and SAW Properties on ALN/Al_2O_3 and ALN/Si," Ultrasonics Symp. Proc., 375 (1981).
9. Handbook of Thin Film Technology, McGraw Hill, New York, N.Y. (1970).
10. J. E. Bowers, "Fiber-Optic Sensor for Surface Acoustic Waves," Appl. Phys. Lett. 41(3), 231, August 1, 1982.

LIST OF FIGURES

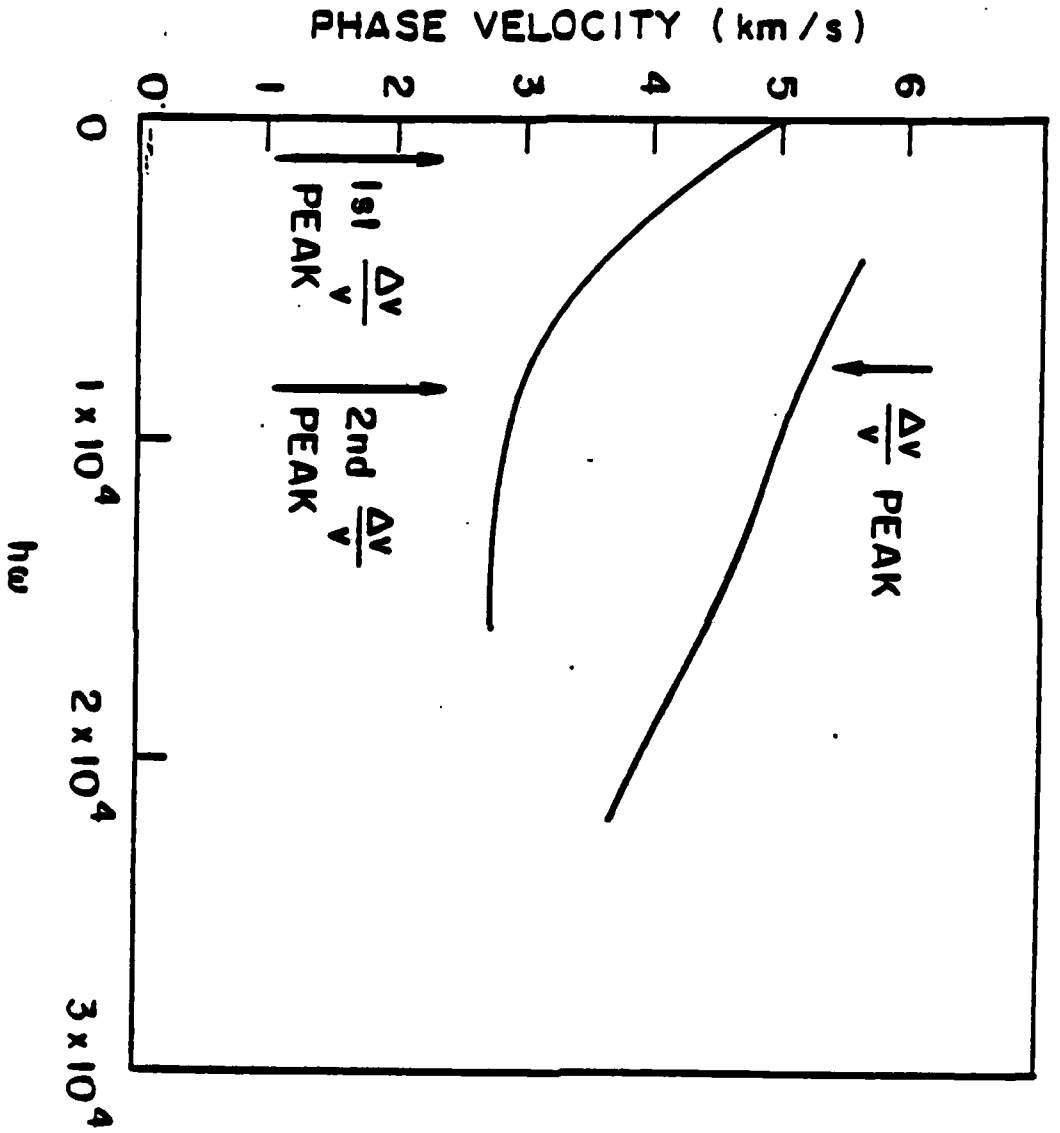
PHASE VELOCITY (km/s)
0
1
2
3
4
5
6
0
1 x 10^4
2 x 10^4
3 x 10^4
hω
1st Δv/v PEAK
2nd Δv/v PEAK
Δv/v PEAK

Fig. 1.

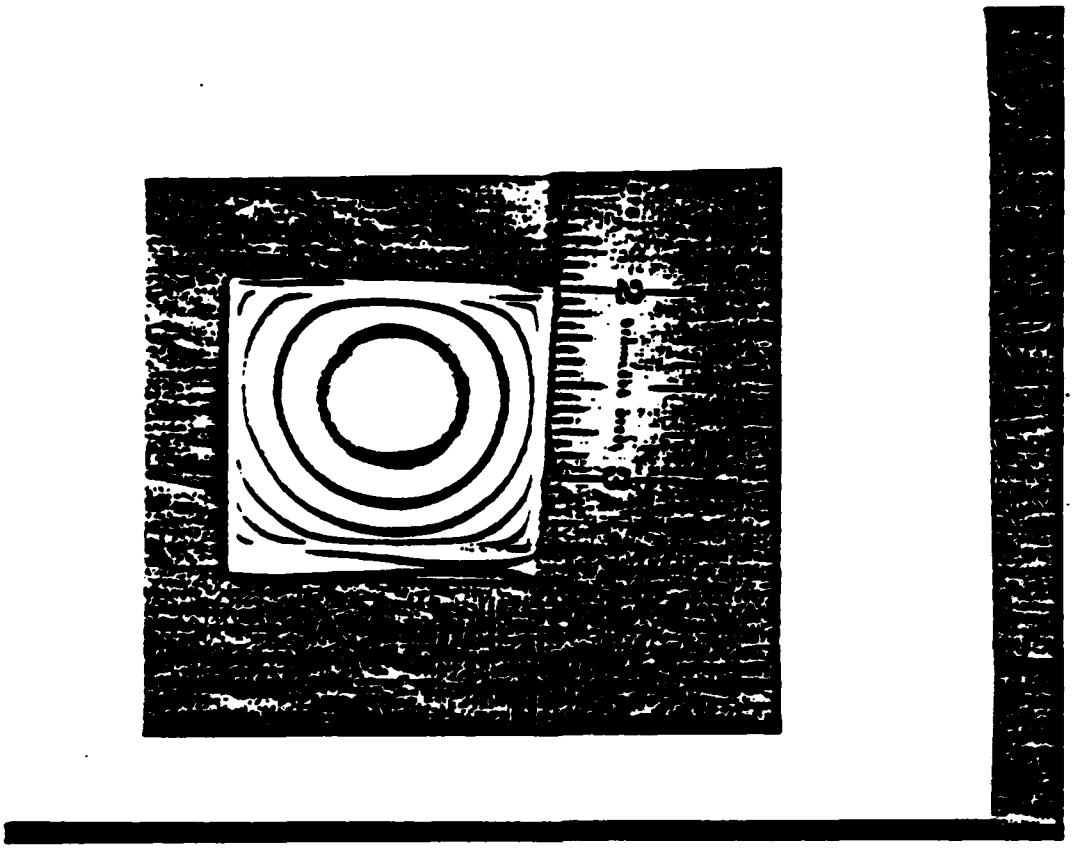

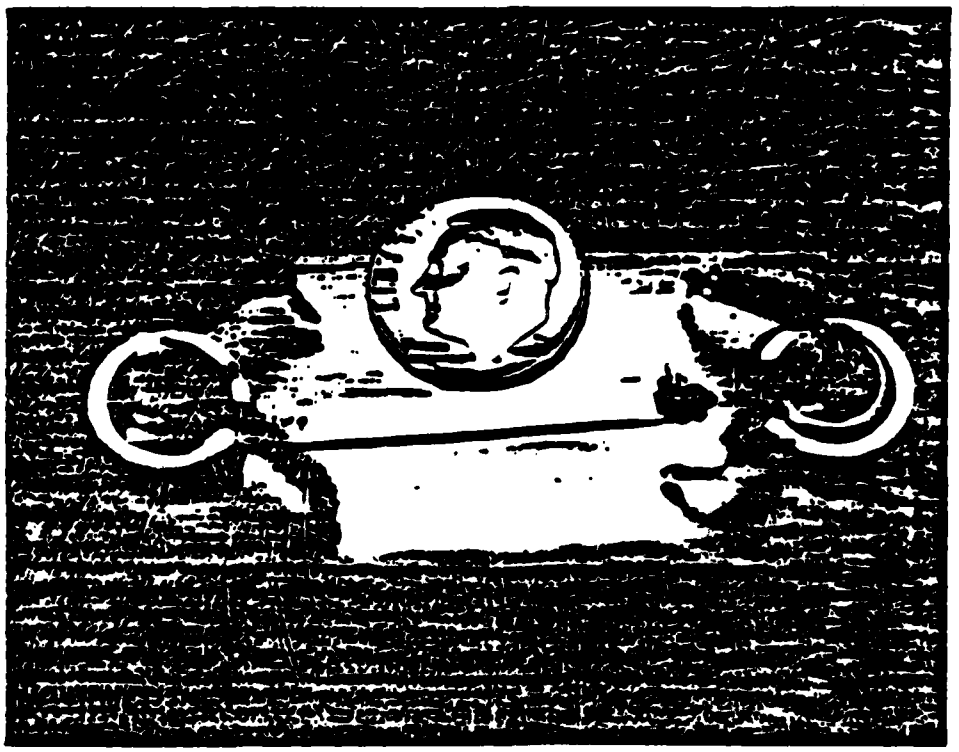

Fig. 2.

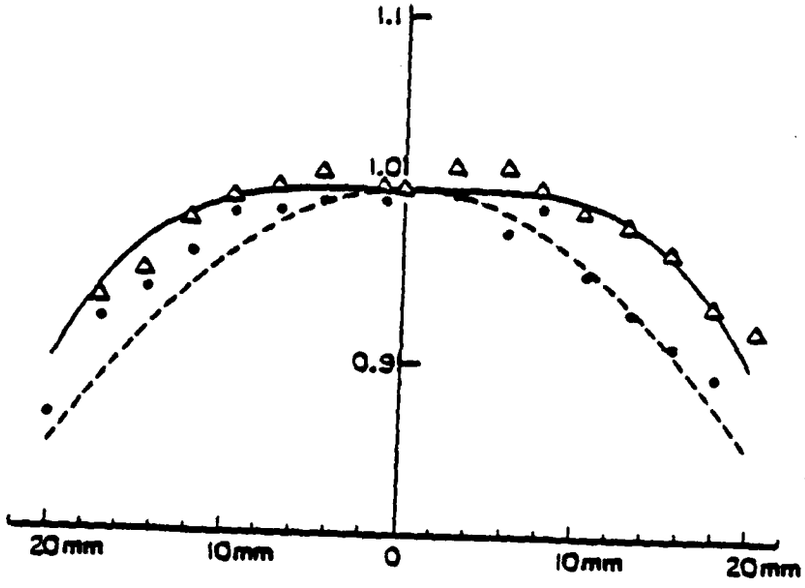

Fig. 3.

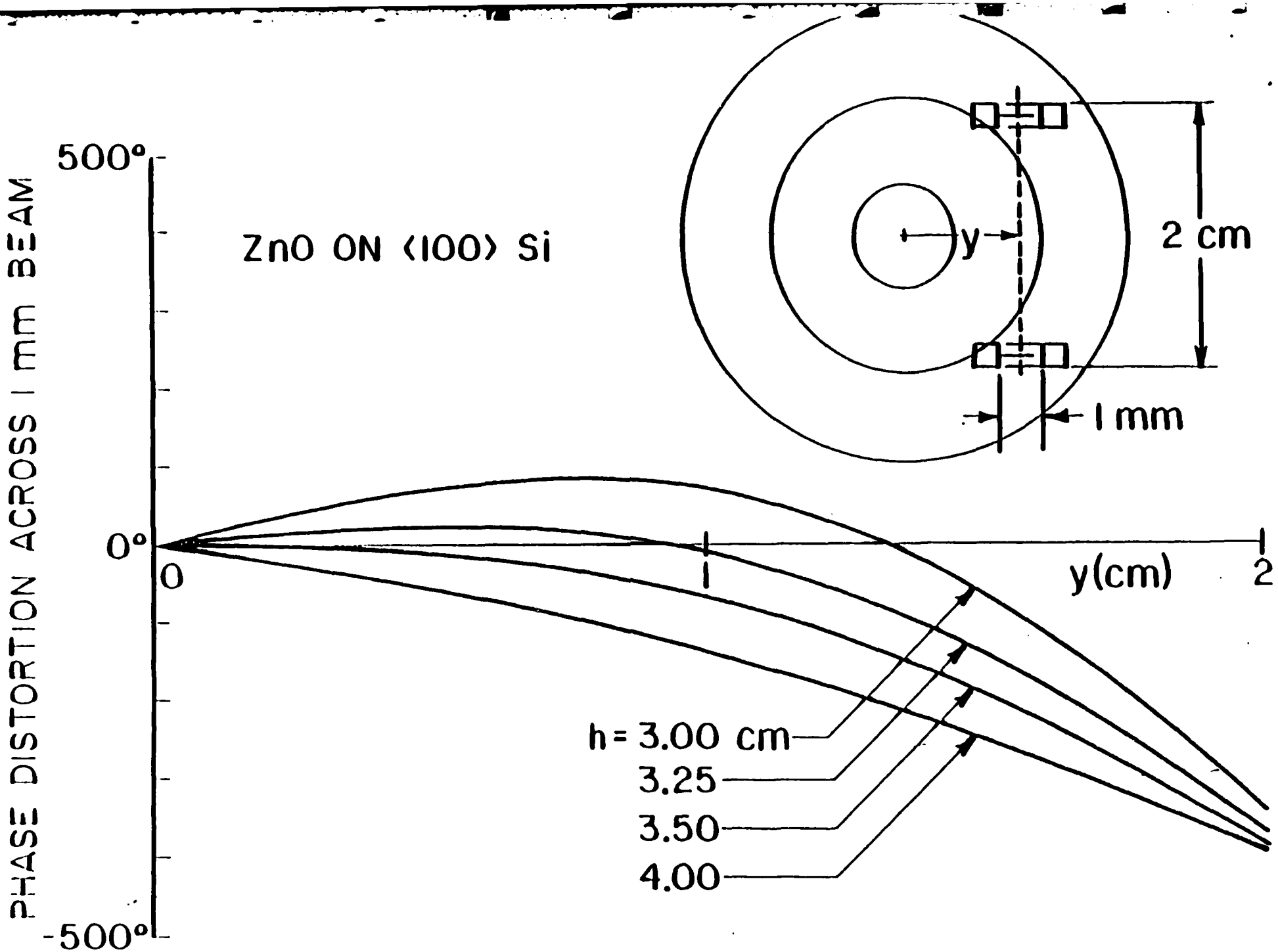
ZnO ON ⟨100⟩ Si
PHASE DISTORTION ACROSS 1 mm BEAM
500°
0°
-500°
0
1
2
y(cm)
y
2 cm
1 mm
h = 3.00 cm
3.25
3.50
4.00

Fig. 4.

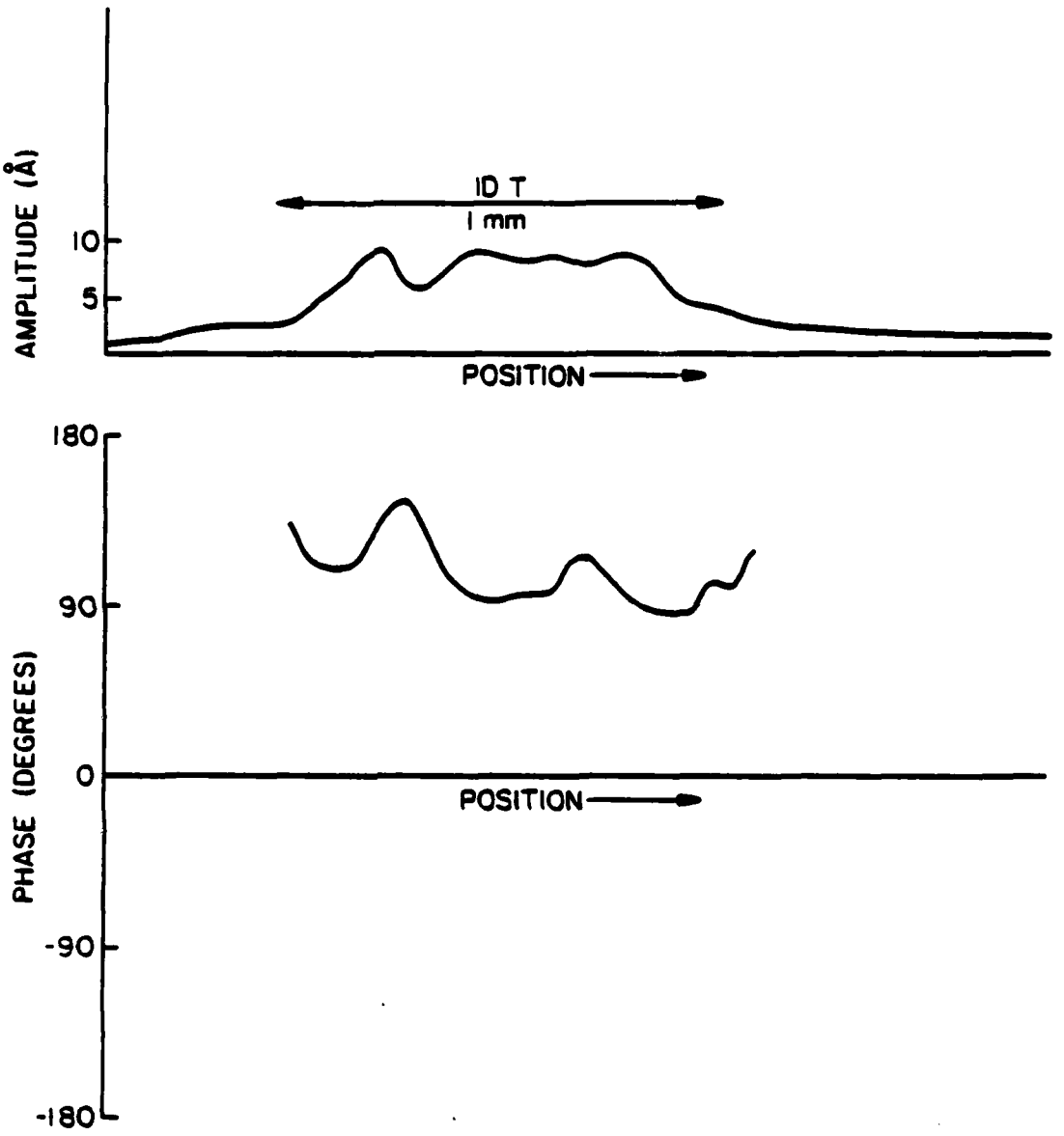
AMPLITUDE (Å)
10
5
1D T
1 mm
POSITION
180
90
0
-90
-180
PHASE (DEGREES)
POSITION

Fig. 5a.

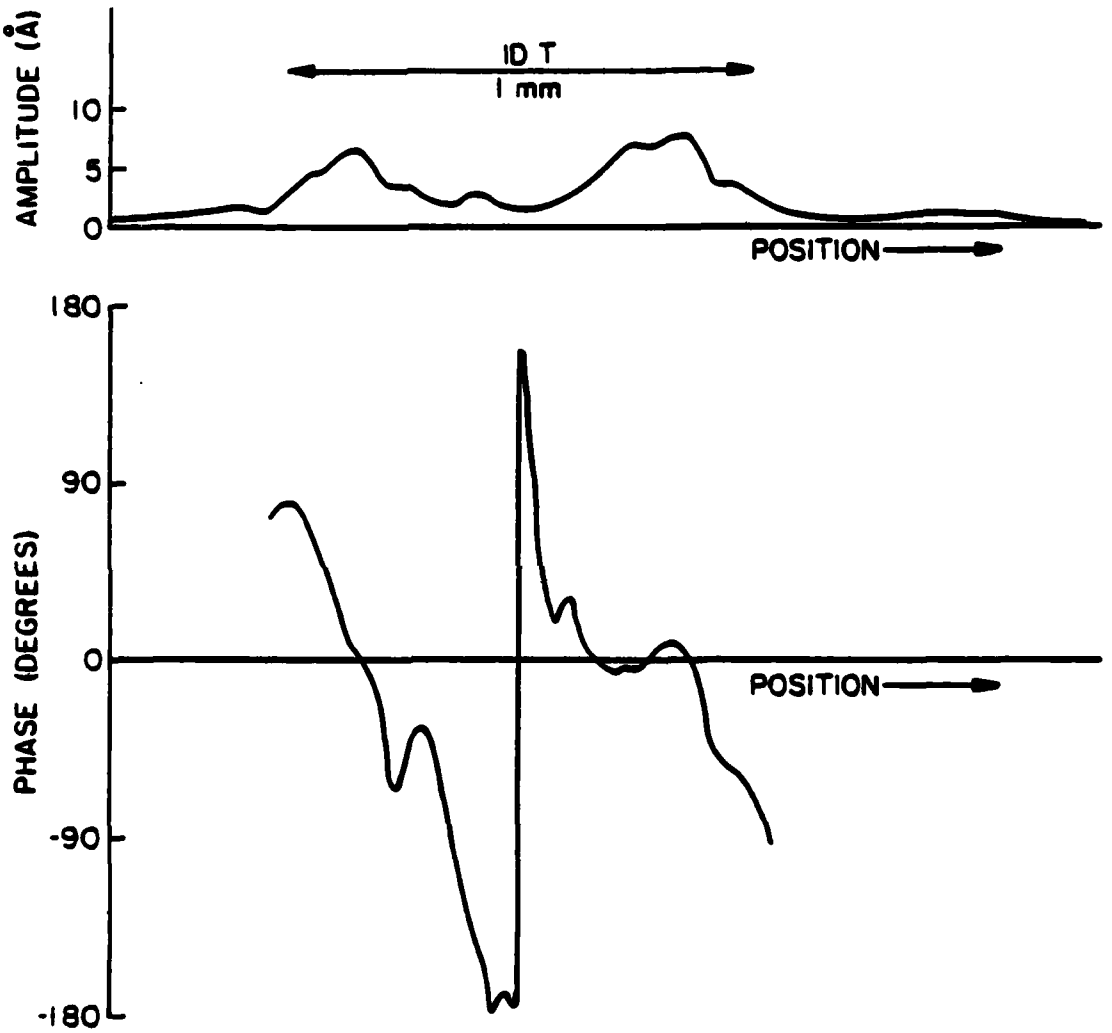
AMPLITUDE (Å)
10
5
0
IDT
1 mm
POSITION
180
90
0
-90
-180
PHASE (DEGREES)
POSITION

Fig. 5b.

NR 243-034

DISTRIBUTION LIST

Addresses	Number of Copies
Director Advanced Research Projects Agency 1400 Wilson Boulevard Arlington, VA 22209 Attention: Program Management	1
Scientific Officer	3
Administrative Contracting Officer	1
Director Naval Research Laboratory Attention: Code 2627 Washington, D.C. 20375	6
Defense Documentation Center Building 5, Cameron Station Alexandria, VA 22314	12
Office of Naval Research (Western Regional Office) 1030 East Green Street Pasadena, California 91101	1
Naval Research Laboratory Code 6850 Washington, D.C. 20375	1
RADC (ETEM) Attn: Dr. P. Carr Hanscom AFB, MA 01731	1
AGED ODDR&E 9th floor 201 Varick Street New York, NY 10014	1
Dr. R. Damon Director, Applied Physics Laboratory Sperry Research Center Sudbury, MA 01776	1

Enclosure (1)

DISTRIBUTION LIST CONTINUED

Addresses	Number of Copies
Dr. R. Wagers Central Research Lab. 13500 North Central Expressway Dallas, Texas 75265	1
Dr. R. Ralston MIT Lincoln Laboratory P.O. Box 73 Lexington, Massachusetts 02173	1
Professor R. Gunshor School of Electrical Engineering Purdue University West Lafayette, Indiana 47907	1